THE JOURNAL OF BIOLOGICAL CHEMISTRY VOL. 285, NO. 28, pp. 21567–21580, July 9, 2010

The B56γ3 Regulatory Subunit of Protein Phosphatase 2A (PP2A) Regulates S Phase-specific Nuclear Accumulation of PP2A and the G_1 to S Transition*[S]

Received for publication, December 15, 2009, and in revised form, May 5, 2010 Published, JBC Papers in Press, May 6, 2010, DOI 10.1074/jbc.M109.094953

Ting-Yuan Lee[‡], Tai-Yu Lai[‡], Shin-Chih Lin[§], Cheng-Wei Wu[§], In-Fan Ni[§], Yu-San Yang[§], Liang-Yi Hung[¶‖], Brian K. Law[**], and Chi-Wu Chiang[‡§‖1]

*From the [‡]Institute of Basic Medical Sciences, [§]Institute of Molecular Medicine, [¶]Institute of Biosignal Transduction, and [‖]Center for Gene Regulation and Signal Transduction Research, College of Medicine, National Cheng Kung University, Tainan 701, Taiwan and the **Department of Pharmacology and Therapeutics, Shands Cancer Center, University of Florida, Gainesville, Florida 32610*

Protein phosphatase 2A (PP2A) is a heterotrimeric enzyme consisting of a scaffold subunit (A), a catalytic subunit (C), and a variable regulatory subunit (B). The regulatory B subunits determine the substrate specificity and subcellular localization of the PP2A holoenzyme. Here, we demonstrate that the subcellular localization of the B56γ3 regulatory subunit is regulated in a cell cycle-specific manner. Notably, B56γ3 becomes enriched in the nucleus at the G_1/S border and in S phase. The S phase-specific nuclear enrichment of B56γ3 is accompanied by increases of nuclear A and C subunits and nuclear PP2A activity. Overexpression of B56γ3 promotes nuclear localization of the A and C subunits, whereas silencing both B56γ2 and B56γ3 blocks the S phase-specific increase in the nuclear localization and activity of PP2A. In NIH3T3 cells, B56γ3 overexpression reduces p27 phosphorylation at Thr-187, concomitantly elevates p27 protein levels, delays the G_1 to S transition, and retards cell proliferation. Consistently, knockdown of endogenous B56γ3 expression reduces p27 protein levels and increases cell proliferation in HeLa cells. These findings demonstrate that the dynamic nuclear distribution of the B56γ3 regulatory subunit controls nuclear PP2A activity, which regulates cell cycle controllers, such as p27, to restrain cell cycle progression, and may be responsible for the tumor suppressor function of PP2A.

Protein phosphatase 2A (PP2A)[2] is one of the major serine/threonine protein phosphatases in mammalian cells and plays a central role in regulating many aspects of cellular functions (1). The PP2A heterotrimeric holoenzyme consists of a dimeric core enzyme, including the catalytic subunit C (PP2A/C) and the structural subunit A (PP2A/A) and a variable regulatory subunit B (PP2A/B). It has been believed that diverse B regulatory subunits target PP2A holoenzymes to specific cellular compartments and determine the substrate specificity of PP2A holoenzymes. Four distinct subfamilies of the regulatory subunit B have been identified, including B (B55 or PR55) (2, 3), B′ (B56 or PR61) (4, 5), B″ (PR72) (6), and B‴ (PR93/PR110) (7). Diverse B subunits are expressed in a developmental- and tissue-specific manner and have distinct subcellular localizations (1, 8, 9). In the mammalian B55 subfamily, B55α, B55β, and B55δ are primarily cytosolic, and B55γ is enriched in the cytoskeletal fraction in neurons (8, 10). Bβ2, one of B55β isoforms, was shown to possess a mitochondrial import signal and target the PP2A holoenzyme to mitochondria (11). Members of the B56 subfamily also reside in distinct subcellular localizations. Murine B56γ1 was shown to associate and colocalize with the focal adhesion regulatory protein paxillin at focal adhesions (12). Human B56α, B56β, and B56ϵ were found to localize mainly to the cytoplasm, but B56γ1, B56γ3, and B56δ were concentrated in the nucleus (13, 14). In addition, B56γ1 was shown to be concentrated in the intranuclear structure known as nuclear speckles in rat cardiomyocytes (15). Furthermore, several isoforms of the B56 subfamily were shown to associate with shugoshin in the centromere and to be involved in PP2A protection of cohesin at centromeres during mitosis in human cells (16, 17).

The dynamic localization patterns of the B regulatory subunits throughout the cell cycle have been intensely studied in yeast. In fission yeast *Schizosaccharomyces pombe,* the intracellular distribution of the B′ subunit Par1p was found to be primarily cytoplasmic but concentrated at the cell center at late stages of mitosis (18). On the other hand, another B′ subunit Par2p showed localization at cell ends during interphase and was found to form a medial ring in cells that are undergoing septation and cytokinesis (18). Furthermore, in the budding yeast *Saccharomyces cerevisiae*, the B regulatory subunits, CDC55 (B type) and RTS1 (B′ type), displayed dynamic and distinct patterns of subcellular localization at the nucleus, bud tip, kinetochore, and bud neck throughout the mitotic cell cycle and to dictate sites of PP2A accumulation (19).

To investigate whether the mammalian B regulatory subunits exhibit dynamic distribution patterns throughout the cell cycle and whether the dynamics of subcellular localization of B regulatory subunits coincide with the localization of PP2A, we

* This work was supported by National Science Council Grants 96-2320-B006-045-MY3 and DOH99-TD-C-111-003 (to the Comprehensive Cancer Center in southern Taiwan).

[S] The on-line version of this article (available at http://www.jbc.org) contains supplemental Figs. 1–4.

[1] To whom correspondence should be addressed: Institute of Molecular Medicine, National Cheng Kung University, No.1 University Rd., 701 Tainan, Taiwan. Tel.: 886-6-235-3535 (ext. 3637); Fax: 886-6-209-5845; E-mail: chiangcw@mail.ncku.edu.tw.

[2] The abbreviations used are: PP2A, protein phosphatase 2A; PBS, phosphate-buffered saline; HA, hemagglutinin; GST, glutathione *S*-transferase; PI, propidium iodide; BS, bovine serum; shRNA, short hairpin RNA.

investigated the subcellular localization of the human B56γ3 subunit throughout the cell cycle. B56γ3, the largest of the B56γ splice variants, displays predominantly nuclear localization when transiently expressed (13, 14). B56γ3 plays a key role in protecting cells from SV40 small t antigen-mediated transformation (20) and targets the PP2A holoenzyme to regulate p53 stability during DNA damage (21, 22). By cell cycle synchronization experiments, we demonstrate that intracellular localization of B56γ3 changes throughout the cell cycle and that, in particular, B56γ3 is markedly increased in the nucleus at the G_1-S boundary and during S phase. Enrichment of B56γ3 in the nucleus is concomitant with increased distribution of the PP2A A and C subunits and PP2A activity in the nucleus. Analyses for the function of B56γ3 on cell cycle indicate a role of B56γ3 in regulating the p27KIP1 protein levels in the G_1 to S phase transition of the cell cycle, and B56γ3 overexpression delayed transition from G_1 to S phase. Together, our data provide further evidence supporting the notion that diverse B regulatory subunits control the subcellular localization of PP2A holoenzymes and PP2A activity in a highly dynamic manner.

EXPERIMENTAL PROCEDURES

Antibodies and Reagents—Antibodies employed include: mouse monoclonal anti-HA tag (6E2) and anti-lamin A/C from Cell Signaling; anti-PP2A/Aα (C-20) from Santa Cruz; anti-PP2A/Cα and anti-p27 from BD Transduction Laboratories; anti-α-tubulin, clone DM1A, and anti-phospho-Kip1 (Thr-187) from Upstate; anti-β-actin and anti-FLAG (M2) from Sigma; anti-HA tag monoclonal antibody (HA.11) and anti-PP2A/Aα (6F9) from Covance; anti-GST antibody from GE Healthcare. All secondary antibodies were from Jackson ImmunoResearch. Serine/threonine phosphatase inhibitor okadaic acid was from Alexis Biochemicals. Protease inhibitors, phenylmethylsulfonyl fluoride, aprotinin, and leupeptin, and propidium iodide (PI) were from Sigma. 4′,6-Diamidino-2-phenylindole dihydrochloride was from Molecular Probes. Lipofectamine 2000 was from Invitrogen. The rabbit anti-B56γ polyclonal antibody (M880) was kindly provided by Dr. Marc Mumby (University of Texas Southwestern Medical Center, Dallas, TX). The pBMN-IRES-EGFP-FLAG-p27 was a gift from Dr. Carlos Arteaga (Vanderbilt University Medical Center, Nashville, TN).

Cell Culture, Cell Lines, and Transfection—NIH3T3 cells were cultured in Dulbecco's modified Eagle's medium supplemented with 10% bovine serum (BS). HeLa cells were cultured in minimum essential medium supplemented with 10% fetal bovine serum. In serum starvation experiments, NIH3T3 cells were grown in medium containing 0.5% BS for 72 h and changed medium every day then were stimulated with 10% BS-containing medium. In proliferation assays, cells were seeded onto 24-well plates, and cell numbers were directly counted. Viability was measured by trypan blue exclusion. A polyclonal pool of cells stably expressing HA-tagged B56γ3 or vector only were created by retroviral infection and subsequent drug selection (usually more than 80% survival) as previously described (23). A pool of cells stably expressing B56γ3-specific shRNA, shRNA targeting both B56γ2 and B56γ3, or shLuc was established with infection and subsequently drug selection using retroviruses made from co-transfection of lentiviral-based expression vector pLKO.1-puro harboring a specific shRNA-encoding sequence, packaging plasmid pCMV-R8.91, and pVSV-G into 293T cells. The retroviral constructs pLKO.1-puro harboring B56γ3-specific shRNA (TRCN0000002495), shRNA for B56γ2 and B56γ3 (TRCN0000002497), or shLuc (TRCN00000072244) were obtained from the National RNAi Core Facility (Institute of Molecular Biology/Genomic Research Center, Academia Sinica, Taiwan). Transient transfection experiments were carried out by co-transfecting NIH3T3 cells with pcDNA3.1–4HAB56γ3 and pBMN-IRES-EGFP-FLAG-p27 or empty vector by Lipofectamine 2000 according to recommended standard procedures.

Cell Cycle Synchronization—The G_1 phase cells were harvested at 6 h (NIH3T3) and 9 h (HeLa) after releasing into the regular medium after nocodazole (200 ng/ml) treatment for 12 h. The cells synchronized at the G_1/S border were obtained using double thymidine block (24), and cells synchronized in mid-S phase were harvested at 3 h after released in the regular medium after double thymidine block treatment. Cells synchronized in G_2/M phase were collected after 12 h of treatment with 200 ng/ml nocodazole. Cells were washed with phosphate-buffered saline (PBS) once, subsequently fixed in 1 ml 75% ethanol, and incubated on ice at least 30 min. The cells were then subjected to PI staining and flow cytometry analysis for monitoring cell cycle progression.

Subcellular Fractionation, Western Blotting, and Co-immunoprecipitation—Subcellular fractionation was performed according to the procedures described previously (25). Whole cell lysates for Western blotting or co-immunoprecipitation were prepared in radio immunoprecipitation assay buffer or isotonic immunoprecipitation buffer by protocols described before (26). For coimmunoprecipitation experiments of PP2A and p27, cells were treated with 2 mM chemical cross-linker dithiobis[succinimidyl propionate] at room temperature for 30 min before harvesting cell lysates. Immunoprecipitation was then carried out according to protocols described before (26). Briefly, whole cell lysates were incubated with anti-HA (HA.11, Covance) or anti-FLAG (M2)-Sepharose, and the anti-HA or anti-FLAG immunocomplexes were subsequently precipitated with or without protein A/G-Sepharose. Whole cell lysates, cytoplasmic and nuclear extracts, and immunocomplex-containing-Sepharose were then mixed with equal volumes of 2× SDS sample buffer (100 mM Tris-Cl, pH 6.8, 20% glycerol, 0.05% bromphenol blue, 4% SDS, and 40% β-mercaptoethanol) and were subjected to SDS-PAGE and Western blotting. Immunoblots were developed using enhanced chemiluminescence. Results were quantified by densitometry using Alpha Innotech AlphaImager.

Immunofluorescence Staining and Microscopy—After various treatments, cells were washed with PBS three times and fixed by 4% paraformaldehyde/PBS for 15 min followed by permeabilization with 0.1% Triton X-100, PBS for 30 min. Cells were blocked with 5% bovine serum albumin, PBS for 1 h, incubated with primary antibody for 1 h (anti-HA, HA.11, 1:1000; anti-B56γ, 1:500; anti-PP2A/A, 6F9, 1:1000; anti-PP2A/C, 1:1000) followed by incubation with the Cy3-conjugated secondary antibody at 1:250 dilution for 1 h. Cells were subsequently stained with 4′,6-diamidino-2-phenylindole dihydro-

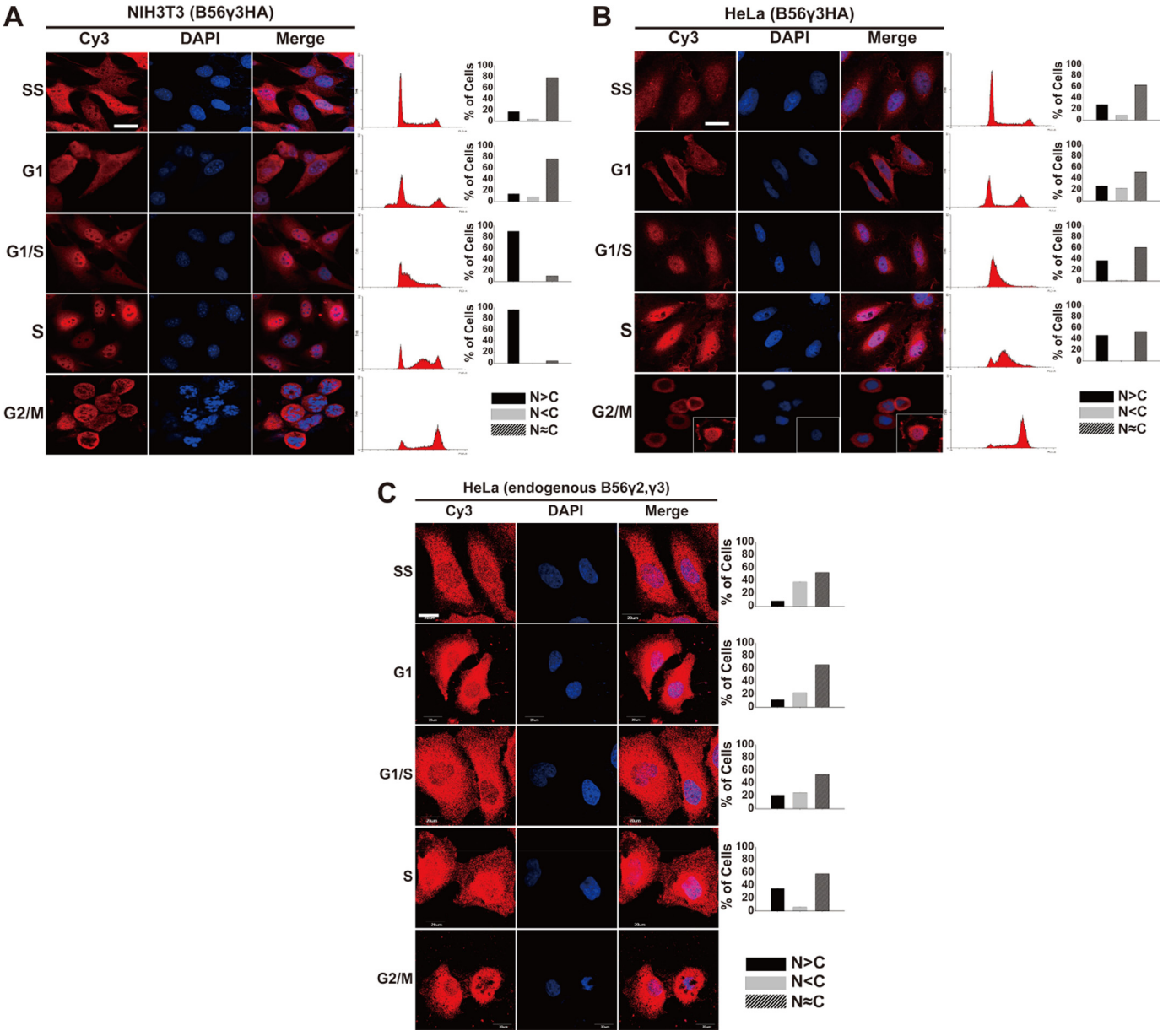

FIGURE 1. **B56γ3 is enriched in the nucleus in a cell cycle-specific manner.** Expression of B56γ3HA in polyclonal pools of NIH3T3 (*A*) and HeLa cells (*B*) stably expressing B56γ3HA or expression of the endogenous B56γ3 in HeLa cells (*C*) was assessed using indirect immunofluorescence with mouse monoclonal anti-HA antibody (*A* and *B*) or a rabbit polyclonal anti-B56γ antibody (*C*) and subsequently detected with Cy3-conjugated anti-mouse or anti-rabbit secondary antibody, respectively, in cells of steady state (*SS*) and in cells synchronized at indicated cell cycle phases, as described under "Experimental Procedures." The cell cycle profiles indicated by PI staining are shown. The nuclei were visualized by staining with 4′,6-diamidino-2-phenylindole dihydrochloride. Cells with different staining patterns of B56γ3 were scored as follows: predominantly nuclear (N>C), homogenously distributed in both nucleus and cytoplasm (N≈C), and predominantly cytoplasmic (N<C). Graphs show quantitative analysis of B56γ3HA distribution in cells, and at least 200 cells were assessed from random fields. The cell merged in the lower right corner of G_2/M cells of HeLa cells was from another field of the same slide and may represent a G_2 cell displaying co-localization of B56γ3HA and the chromatin. Data shown are from one representative experiment of at least two experiments with similar results. *Scale bar*, 20 μm. *DAPI*, 4′,6-diamidino-2-phenylindole dihydrochloride.

chloride (5 μM) for 5 min. Cells were visualized by fluorescence microcopy (Olympus, BX51) at 200× magnification or confocal microcopy (Olympus, FV1000) at 400× or 600× magnification. Quantification of fluorescence images for subcellular distribution of immunostained proteins was performed by scoring at least 200 cells on slides by dividing staining patterns as predominantly nuclear (N), homogenously nuclear and cytoplasmic (N≈C), and predominantly cytoplasmic (C).

Cell Cycle Analysis—For immunofluorescence staining experiments in synchronized cells, cells were grown on both coverslips and 10-cm dishes. After synchronization treatments, cells on 10-cm dishes were immediately harvested by trypsinization, pelleted by centrifugation, fixed in 75% ethanol, and resuspended in PI buffer (40 μg/ml propidium iodide, 100 μg/ml RNase A in PBS). The DNA content of cells (10,000 cells/sample) was then measured on a FACSCalibur (BD Biosciences). For cell cycle re-entry experiments by serum stimulation, NIH3T3 cells were seeded on 15-cm dishes (7×10^5/dish) in 10% BS-containing medium overnight. Cells were subsequently grown in 0.5% BS-containing medium for 72 h for

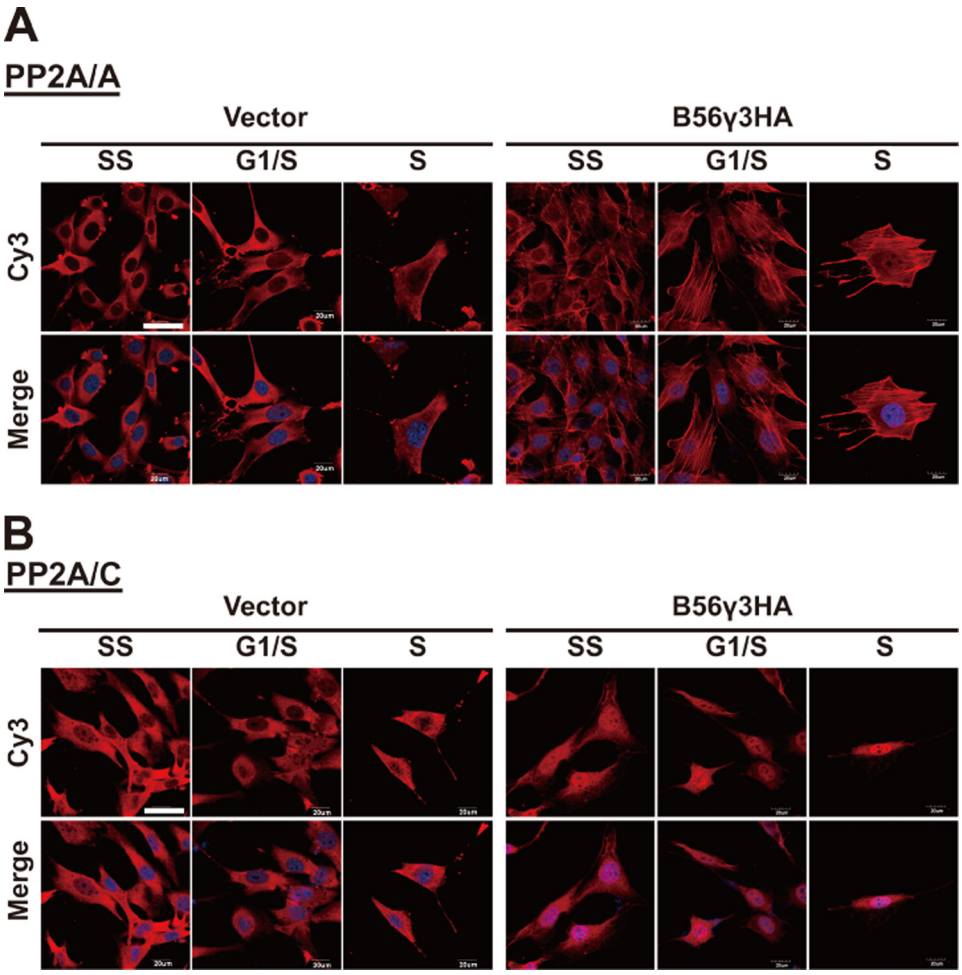

FIGURE 2. **Overexpression of B56γ3 facilitates nuclear localization of PP2A A and C subunits in NIH3T3 cells.** *A* and *B*, the distribution of PP2A A and C subunit, respectively, was visualized in NIH3T3 cells carrying vector only or overexpressing B56γ3HA by indirect immunofluorescence with mouse monoclonal anti-PP2A A or PP2A C subunit antibodies and Cy3-conjugated anti-mouse secondary antibody in cells in steady state (*SS*) and in cells synchronized at the G_1/S border or after entering S phase, as described under "Experimental Procedures." *Scale bar*, 20 μm.

arrest at G_0/G_1 and were replenished with 10% BS-containing medium to induce re-entry into cell cycle. For cell cycle re-entry experiments by release from contact inhibition, cells were grown to confluence and were then trypsinized and replated with a low density. Cells were collected at various time points after re-addition of 10% serum or replating, fixed with cold 70% ethanol, and subjected to flow cytometry analysis as described earlier.

Measurement of the PP2A Activity—PP2A activity was measured using a PP2A DuoSet IC kit (R&D Systems) with some modifications. Briefly, whole cell lysates were prepared in ice-cold lysis buffer (50 mM HEPES, pH 7.5, 0.1 mM EGTA, 0.1 mM EDTA, 120 mM NaCl, 0.5% Nonidet P-40, 25 μg/ml pepstatin, 1 mM phenylmethylsulfonyl fluoride, 2 μg/ml aprotinin, 25 μg/ml leupeptin), and subsequently aliquots (75 μg) of cell lysates, extracts of cytoplasm, or extracts of the nucleus prepared as described earlier were loaded onto 96-well plates coated with a capture antibody specific for the C subunit for immunocapture at 4 °C for 3 h. After washing twice, synthetic phosphopeptide substrates (200 μM) were added for the dephosphorylation reaction catalyzed by PP2A. The level of free phosphate was determined by measuring the absorbance at 620 nm by a dye binding assay using malachite green and molybdic acid.

In Vitro Pulldown Analysis—The recombinant His-B56γ3, GST, and GST-p27 proteins were prepared by following the protocols described before (23) using *Escherichia coli* BL21 cells harboring the expression construct including pQE30-His(6)-B56γ3-HA, pGEX-4T-1, or pGEX-4T-p27. For analyzing direct interactions of B56γ3 and p27 *in vitro*, 2 μg of purified recombinant GST or GST-p27 proteins were incubated with 2 μg of purified recombinant His-B56γ3 proteins in pulldown buffer (1× PBS with 0.2% Triton X-100) for 4 h at 4 °C. GST fusion proteins were pulled down by glutathione-Sepharose 4B, washed five times with pulldown buffer, fractionated by SDS-PAGE, and analyzed by Western blotting with anti-B56γ or anti-GST antibody as described earlier.

In Vitro p27 Dephosphorylation Analysis—FLAG-tagged p27 was immunoprecipitated from NIH3T3 cells transfected with pBMN-IRES-EGFP-FLAG-p27 48 h after transfection by protocols described before (26). The PP2A B56γ3 holoenzymes were prepared from NIH3T3 cells stably expressing HA-tagged B56γ3 by immunoprecipitation using anti-HA antibody and precipitated by protein A-Sepharose. The FLAG-tagged p27 or B56γ3 immunocomplexes were then resuspended in the phosphatase assay buffer (20 mM imidazole, 150 mM NaCl, 14.4 mM β-mercaptoethanol, 1 mM phenylmethylsulfonyl fluoride, 10 μg/ml aprotinin, and 10 μg/ml leupeptin). Aliquots of p27 immunocomplexes were then mixed with various amounts of B56γ3 immunocomplexes and incubated at 30 °C for 30 min. Dephosphorylation reactions were terminated by adding 4× SDS sample buffer and boiling for 5 min.

RESULTS

The Subcellular Distribution of the B56γ3 Subunit Is Regulated in a Cell Cycle-dependent Manner—We first investigated the subcellular localization of B56γ3 in a pool of NIH3T3 cells stably expressing HA-tagged B56γ3 (B56γ3HA) throughout the cell cycle. Immunofluorescence staining (Fig. 1*A*) showed that B56γ3HA was ubiquitously distributed throughout the entire cell in most NIH3T3 cells in steady-state asynchronous populations. When NIH3T3 cells were synchronized in the G_1 phase after several hours after release from treatment with

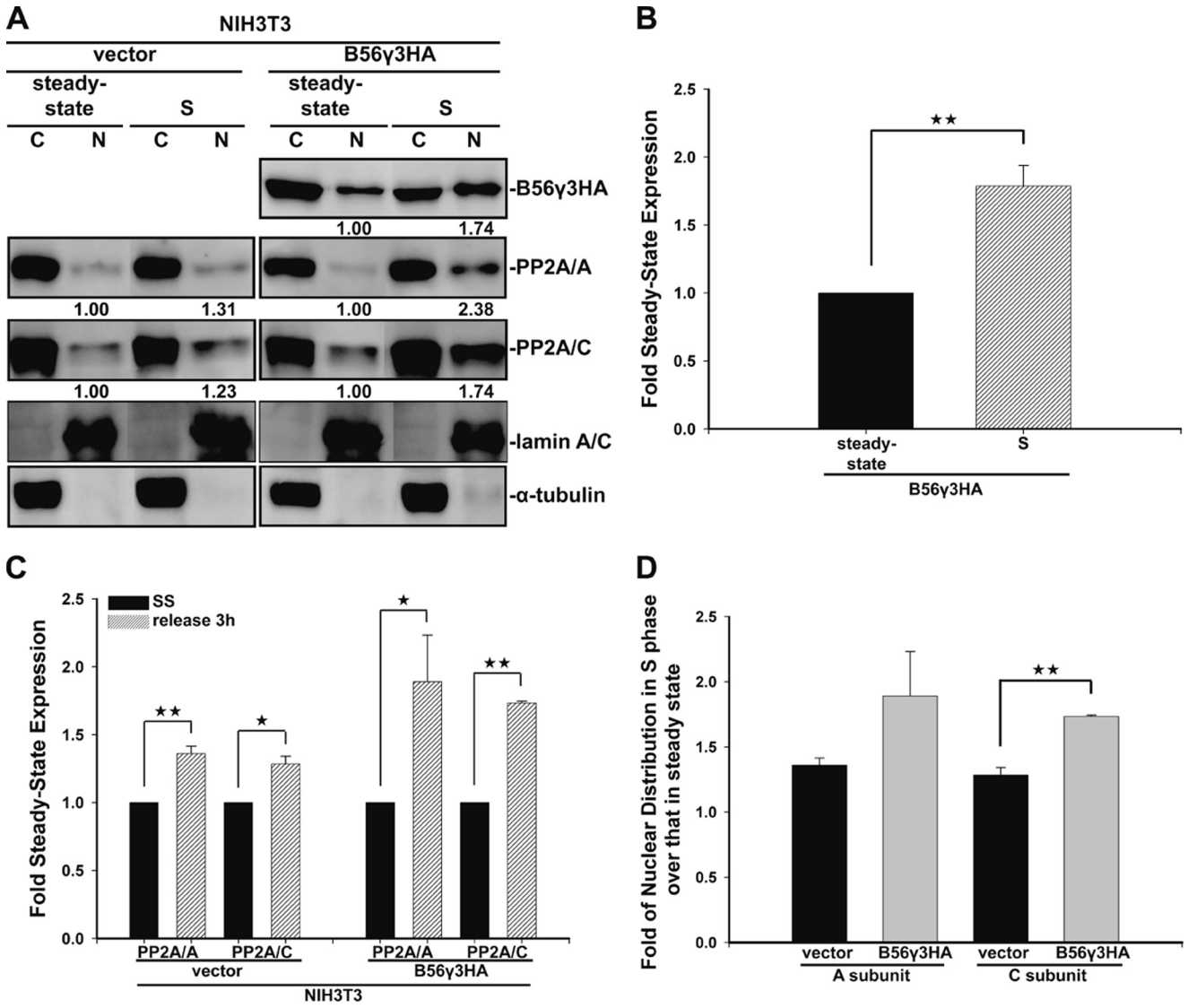

FIGURE 3. **Subcellular fractionation analyses demonstrate S phase-specific increase of nuclear localization of PP2A A, B56γ3, and C subunits.** Whole cell lysates of NIH3T3 cells of steady state or 3 h released from double thymidine block treatment (S phase) were fractionated as described under "Experimental Procedures." *A*, portions of cytoplasmic (*C*) and nuclear (*N*) fractions were analyzed by SDS-PAGE and Western blotting for expression levels of PP2A A, B56γ3HA, and C subunits. α-Tubulin and lamin A/C were used as cytoplasmic and nuclear markers, respectively. The relative expression levels of individual subunits in the nuclear fraction in steady state and S phase were quantified by densitometry and normalized with lamin. The data shown are expressed as -fold expression level over that of steady state, which was set as 1 for individual subunits during progression into S phase. Representative data of three experiments with similar results are shown. *B*, the data show a comparison between nuclear expression levels of B56γ3HA in steady state and in S phase. *C*, the data show comparisons between expression levels of the nuclear A or C subunit in steady state (*SS*) and that in S phase in vector only or B56γ3HA-overexpressing cells. *D*, the data show comparisons between S phase-specific increase of the nuclear A or C subunit in vector only and that in B56γ3HA-overexpressing cells. The differences were assessed for statistical significance by Student's *t* test with *p* value < 0.05 (*) or < 0.005 (**).

nocodazole, the distribution of B56γ3HA was mostly ubiquitous. When cells were arrested at the border between G_1 and S phase by double thymidine block, we found that staining of B56γ3HA was markedly enriched in the nucleus (Fig. 1*A*). When most cells entered mid-S phase 3 h after release from double thymidine block, staining of B56γ3HA was further enriched in the nucleus (Fig. 1*A*). Furthermore, B56γ3HA was concentrated at the area surrounding but not overlapping the chromatin in cells arrested in G_2/M by nocodazole treatment (Fig. 1*A*). In contrast, we did not observe a similar cell cycle-specific nuclear accumulation pattern when B55α and B56α were investigated (data not shown). To investigate whether the findings are unique to NIH3T3 cells, we investigated the distribution of B56γ3HA in HeLa cells. The distribution pattern of B56γ3HA in HeLa cells was similar to that of NIH3T3 cells in both asynchronous cells and in synchronized cells (Fig. 1*B*). However, we observed that there were more HeLa cells exhibiting primarily nuclear and perinuclear staining of B56γ3HA in steady state compared with NIH3T3 cells. In addition, the level of enrichment in nuclear staining of B56γ3HA during progression into S phase was lower than that of NIH3T3 cells, and some cells exhibited staining of B56γ3HA that overlapped with the chromatin (Fig. 1*B*). To further confirm that our finding of distribution of stably expressed exogenous B56γ3 also applied to the endogenous B56γ3, we studied the distribution of the endogenous B56γ subunits (B56γ2 and B56γ3) in HeLa cells by immunostaining using a polyclonal antibody against an epitope at the C terminus of both human B56γ2 and B56γ3. The overall

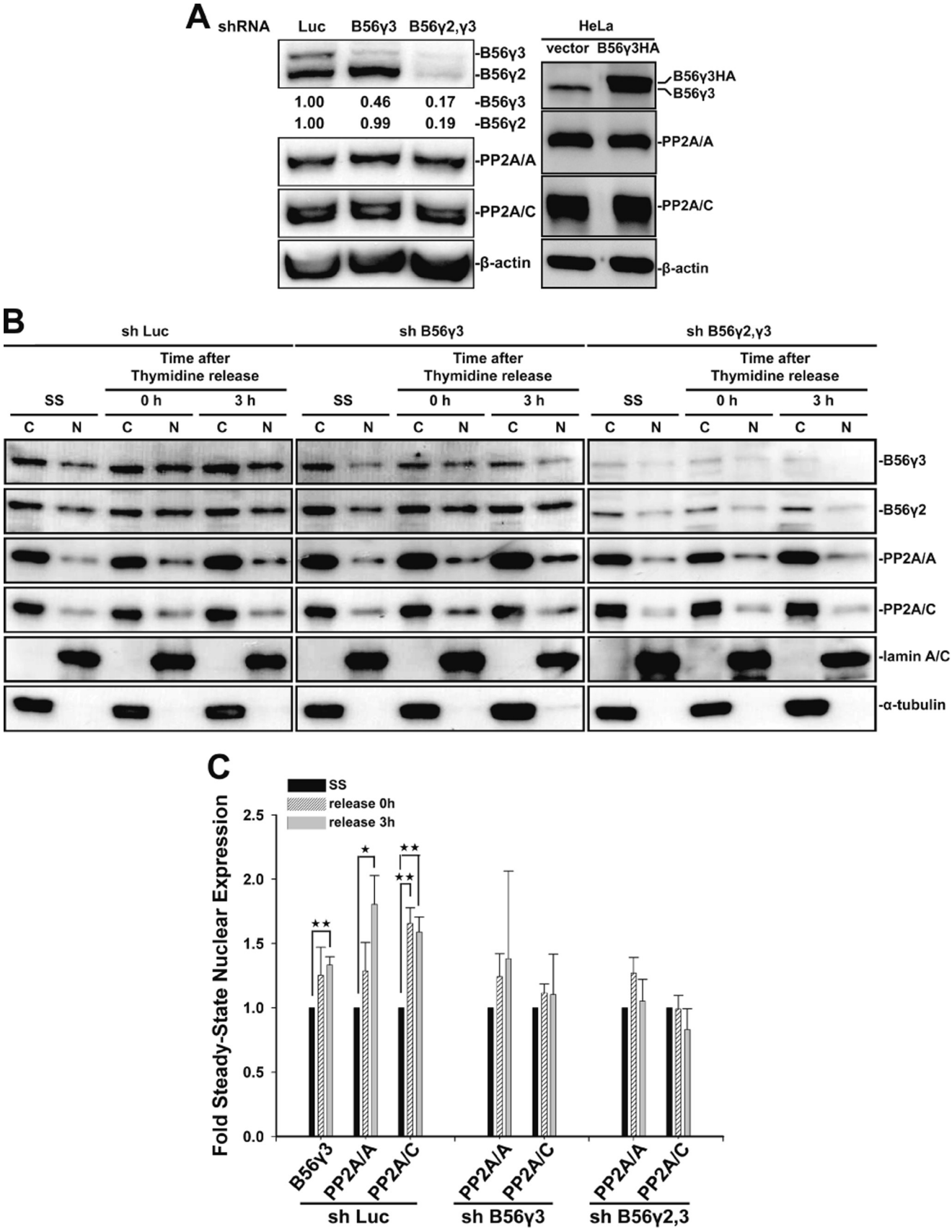
A
shRNA
Luc
B56γ3
B56γ2,γ3
HeLa
vector
B56γ3HA
-B56γ3
-B56γ2
1.00
0.46
0.17
-B56γ3
1.00
0.99
0.19
-B56γ2
-PP2A/A
-PP2A/C
-β-actin
B56γ3HA
B56γ3
-PP2A/A
-PP2A/C
-β-actin
B
sh Luc
sh B56γ3
sh B56γ2,γ3
Time after Thymidine release
SS
0 h
3 h
C
N
-B56γ3
-B56γ2
-PP2A/A
-PP2A/C
-lamin A/C
-α-tubulin
C
SS
release 0h
release 3h
Fold Steady-State Nuclear Expression
2.5
2.0
1.5
1.0
0.5
0.0
B56γ3
PP2A/A
PP2A/C
PP2A/A
PP2A/C
PP2A/A
PP2A/C
sh Luc
sh B56γ3
sh B56γ2,3

distribution pattern of the endogenous B56γ subunits in HeLa cells (Fig. 1*C*) was similar to that of exogenous B56γ3 except for some differences in the level of enrichment in the nucleus. In asynchronous steady-state cells and cells synchronized in G_1 phase, the endogenous B56γ subunits were ubiquitously distributed throughout the entire cells. When cells were synchronized at the G_1/S border, the endogenous B56γ subunits started to accumulate toward the perinuclear area but to a much lesser extent than exogenous B56γ3 (Fig. 1*B*). In cells synchronized in S phase, the endogenous B56γ subunits became highly enriched at the perinuclear area and in the nucleus. In cells synchronized in G_2/M phase, the endogenous B56γ subunits were distributed at the area surrounding the chromatin or overlapping with the chromatin. Furthermore, during investigation of the subcellular localization of B56γ3HA in cells entering G_1 after released from G_2/M arrest, we observed dynamic staining patterns of B56γ3HA localization between the cytoplasm and nucleus through the time course (supplemental Fig. 1). Together, these results suggest that the distribution of B56γ3 is controlled in a cell cycle-dependent manner.

B56γ3 Overexpression Increases Nuclear Localization of the A and C Subunits of PP2A—Given that the regulatory B subunits determine subcellular localization of PP2A holoenzymes and that nuclear distribution of B56γ3HA was markedly increased during entry of S phase (Fig. 1), we examined the distribution of the A and C subunits in steady-state asynchronous cells and in cells progressing into S phase by comparing NIH3T3 cells carrying vector only with cells overexpressing B56γ3HA. We found that staining of the A subunit was primarily cytoplasmic, and overexpression of B56γ3 caused not only an increase in nuclear staining but also a marked increase in filament array staining (Fig. 2*A*). When cells were synchronized at the G_1/S border and in S phase, the nuclear staining of the A subunit was significantly increased in cells overexpressing B56γ3 as compared with the minimal changes found in cells carrying vector only (Fig. 2*A*). Next, we examined staining of the C subunit and found that B56γ3 overexpression resulted in a significantly enhanced nuclear staining of the C subunit in asynchronous cells (Fig. 2*B*). We also noticed that more staining of the C subunit was detected in the nucleus than that of the A subunit in control cells (Fig. 2*B*, *left*). As cells were synchronized at the G_1/S border and in S phase, cells with B56γ3 overexpression still showed more nuclear staining of the C subunit than control cells (Fig. 2*B*). In parallel, we analyzed the impact of B56γ3 overexpression on distribution of the A and C subunits in HeLa cells (supplemental Fig. 2). Similar to NIH3T3 cells, B56γ3 overexpression resulted in an elevated nuclear staining of the A subunit in asynchronous cells and cells progressing into S phase, whereas an enhanced nuclear staining of the C subunit by B56γ3 overexpression was only observed in cells progressing into S phase as compared with cells carrying vector only (supplemental Fig. 2). These results indicate that overexpression of B56γ3 enhances the nuclear localization of the PP2A A and C subunits.

Biochemical Fractionation Reveals S Phase-specific Increases in Nuclear Distribution of B56γ3, A, and C Subunits—The results of fluorescence microscopy analyses showed an S phase-specific elevation in the nuclear staining of B56γ3HA and increased levels of the nuclear staining of the A and C subunits mediated by overexpression of B56γ3. We further performed subcellular fractionation for cell extracts in conjunction with Western blot analysis to confirm and perform quantitative analyses for the findings. We prepared nuclear and cytoplasmic extracts by fractionating total cell lysates of NIH3T3 cells with vector only or B56γ3HA overexpression and analyzed the expression of A, B56γ3HA, and C subunits by SDS-PAGE followed by Western blotting. As expected in NIH3T3 cells, we found a very significant increase, up to 74%, in levels of nuclear B56γ3HA in cells synchronized in S phase compared with that in steady state (Fig. 3, *A*, *right*, and *B*). Increases in both the endogenous A and C subunits in the nuclear fraction were observed in the control cells as cells entered S phase (Fig. 3, *A*, *left*, and *C*). B56γ3 overexpression further enhanced the increase in the A and C subunits (up to 138 and 74%, respectively) (Fig. 3, *A*, *right*, *C*, and *D*) in the nuclear fraction as compared with that of vector only cells (up to 31 and 23%, respectively) (Fig. 3, *A*, *left*, *C*, and *D*) as cells entered S phase. In parallel, we examined the expression levels of the A, B56γ3HA, and C subunits in subcellular fractions of HeLa cells overexpressing B56γ3. Similar to NIH3T3 cells and consistent with results of microscopy analysis, we observed an increase in nuclear B56γ3HA and a modest increase in nuclear A and C subunits mediated by B56γ3 overexpression during progression into S phase (data not shown). Next, we investigated whether endogenous B56γ3 could act similarly to exogenous B56γ3 in the S phase-specific nuclear enrichment and in regulating the nuclear distribution of the A and C subunits when cells progress into S phase. We investigated the role of endogenous B56γ3 in regulating nuclear localization of PP2A in HeLa cells. We fractionated the whole cell extracts from steady-state asynchronous, G_1/S-boundary and S phase-synchronized HeLa cells with control shLuc knockdown, specific shB56γ3 knockdown, or both shB56γ2 and shB56γ3 knockdown (Fig. 4). Consistent with the findings with exogenous B56γ3, endogenous B56γ3 is expressed in both cytoplasm and nucleus (Fig. 4*B*), and similarly, A and C subunits along with B56γ3 were increased in the nuclear fraction upon progression into the S phase (Fig. 4*B*, *left*, and quantified in *C*). When endogenous B56γ3 was specif-

FIGURE 4. **Silencing the endogenous B56γ subunits abolishes S phase-specific increase of nuclear distribution of PP2A A and C subunits.** *A*, efficiency of silencing endogenous B56γ2 and B56γ3 of HeLa cells (*left panel*) by an shRNA specifically targeting B56γ3 or an shRNA to both B56γ2 and B56γ3, respectively, is shown. Expression levels of the A, B56γ3, and C subunits were shown (*right panel*) in both vector only and B56γ3HA-overexpressing HeLa cells by Western blotting. *B*, aliquots of cytoplasmic (*C*) and nuclear (*N*) fractions of HeLa cells with control shLuc knockdown, B56γ3 knockdown, or B56γ2 and B56γ3 knockdown in steady-state cells, 0 h after release from double thymidine block treatment or 3 h after release from double thymidine block treatment were fractionated, analyzed, and quantified for expression levels of PP2A A, B56γ2, B56γ3, and C subunits as described in Fig. 3. Representative data of three experiments with similar results are shown. *SS*, steady state. *C*, data (quantified results in *B*) shown are expressed as -fold expression level over that of steady state, which was set as 1 for individual subunits during progression into S phase. Data are shown as means ± S.D. of three experiments. The differences between various experimental settings and control conditions were assessed for statistical significance by Student's *t* test with p value < 0.05 (*) or < 0.005 (**).

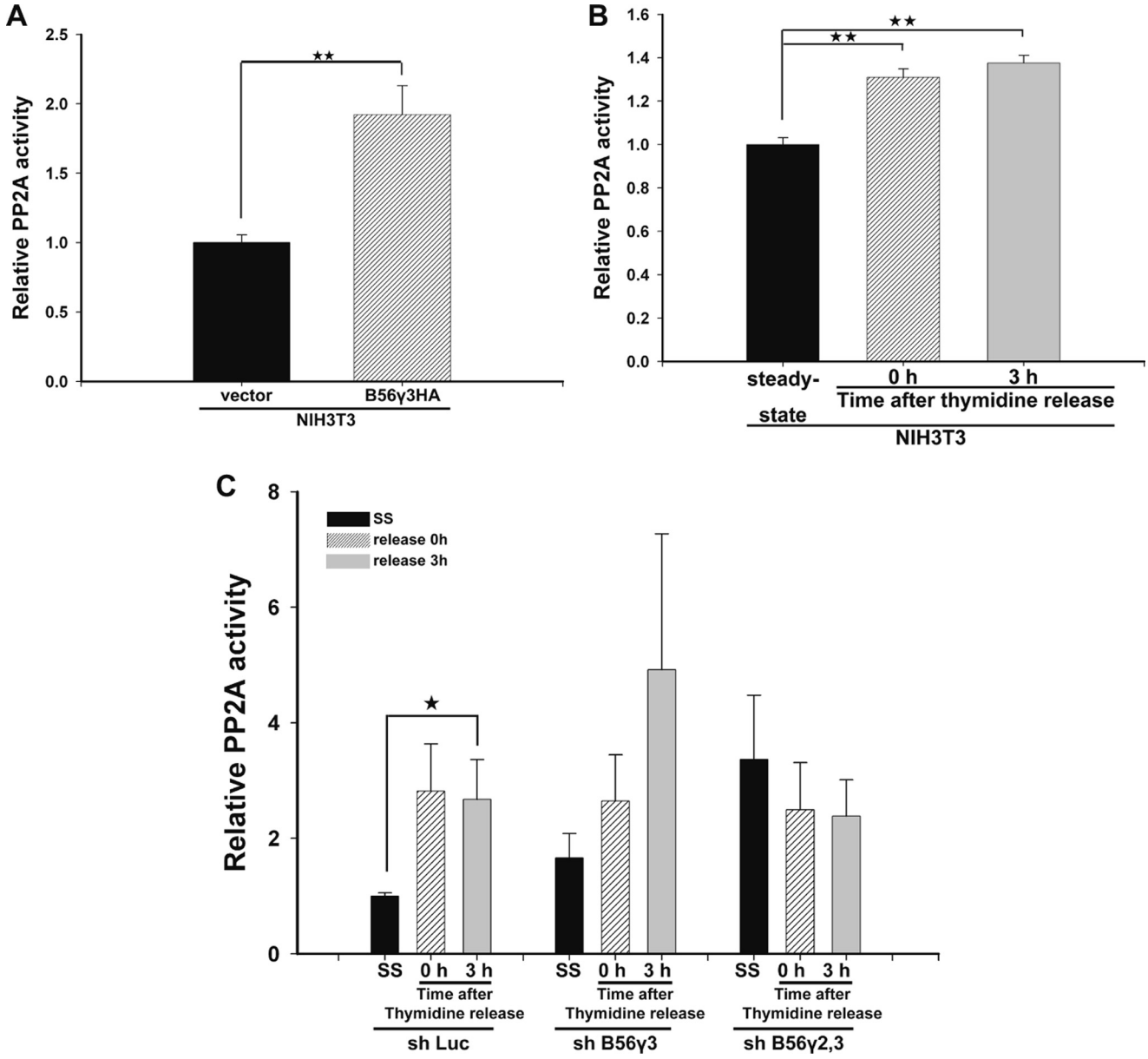

FIGURE 5. **B56γ subunits regulate S phase-specific increase in nuclear PP2A activity.** *A*, PP2A activities of nuclear extracts of NIH3T3 cells with vector only or B56γ3HA overexpression were analyzed as described under "Experimental Procedures." Results were expressed as relative activity *versus* that of cells carrying vector only at steady state (*SS*), which was set as 1. *B*, PP2A activities of nuclear fractions were assessed in the nuclear extracts of NIH3T3 cells with B56γ3HA overexpression at steady state, 0 h after release from double thymidine block, or 3 h after release from double thymidine block. Results were expressed as relative activity *versus* that of cells at steady state, which was set as 1. *C*, PP2A activities of nuclear fractions were assessed in the nuclear extracts of HeLa cells with control shRNA (shLuc) knockdown, B56γ3 knockdown, or B56γ2 and B56γ3 knockdown at steady state, 0 h released from double thymidine block treatment, or 3 h released from double thymidine block treatment. Results were expressed as relative activity *versus* that of cells with control shLuc knockdown at steady state, which was set as 1. Data are shown as means ± S.E. of at least three experiments. The differences between various experimental settings and control conditions were assessed for statistical significance by Student's *t* test with p value < 0.05 (*) or < 0.005 (**).

ically knocked down (near 60% reduction) (Fig. 4, *A* and *B*, *middle*), the levels of increase in nuclear A and C subunits were substantially reduced in S phase as compared with that in control shLuc knockdown cells (Fig. 4*B*, *middle*, and quantified in *C*). Although the levels of increase in nuclear A and C subunits were substantially reduced due to B56γ3 knockdown when cells entered S phase, we noticed that there was a significant variation in levels of increased A and C subunits among experiments (Fig. 4*C*, *middle*). Because the three B56γ splice variants, B56γ1, B56γ2, and B56γ3, share high identity (98%) in amino acid sequences and all variants locate to the nucleus (13, 14), we thought that the other B56γ variants may also participate in regulating the S phase-specific increase in nuclear PP2A holoenzymes and may contribute to this variation. In support of this, levels of B56γ2 were also elevated in the nucleus during progression into S phase (Fig. 4*B*). We addressed this issue by employing another shRNA construct that targeted to both B56γ2 and B56γ3 and showed a higher efficiency in silencing both B56γ2 and B56γ3 expression (near 80% reduction) (Fig. 4, *A* and *B*, *right*). As shown in Fig. 4, *B* and *C*, when expression of both B56γ2 and B56γ3 was more efficiently knocked down, the increases in nuclear A and C subunits were further reduced

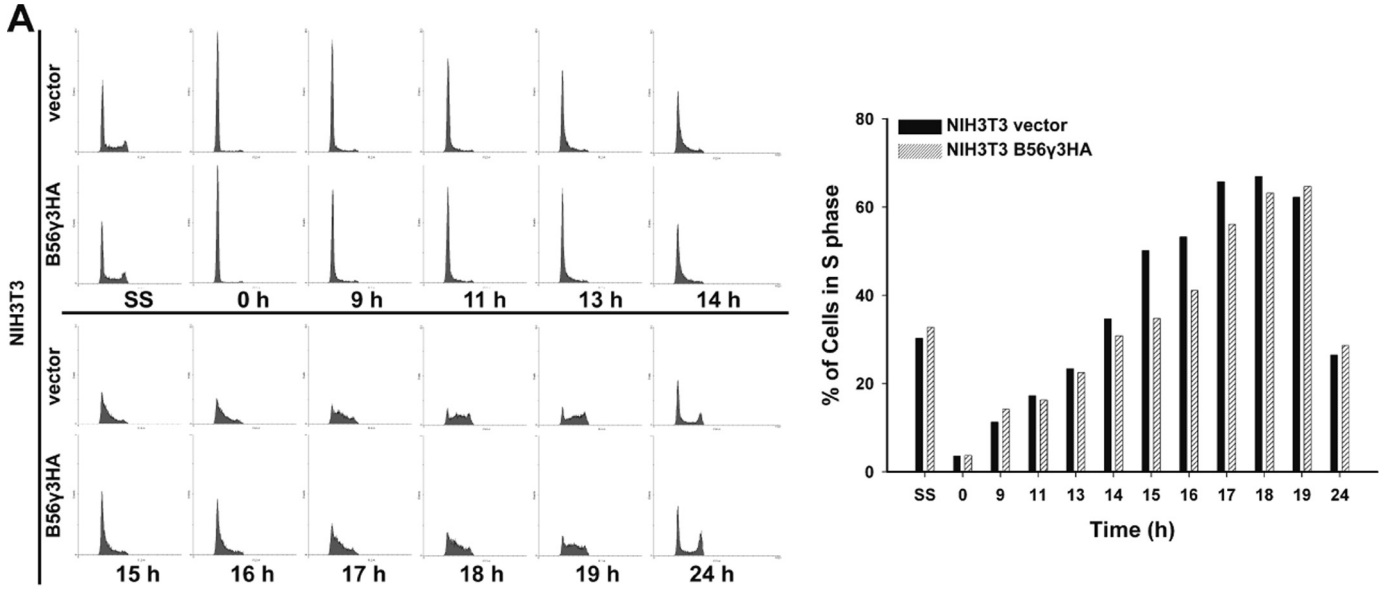
A
NIH3T3
vector
B56γ3HA
SS
0 h
9 h
11 h
13 h
14 h
15 h
16 h
17 h
18 h
19 h
24 h
NIH3T3 vector
NIH3T3 B56γ3HA
% of Cells in S phase
Time (h)

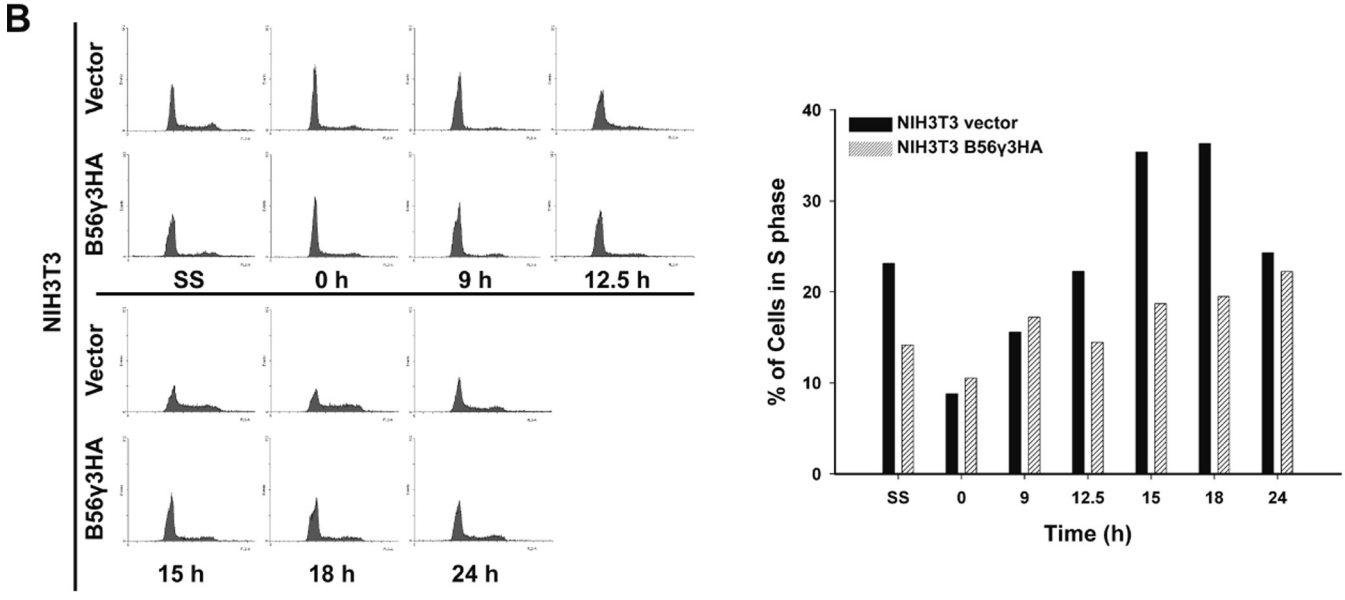
B
NIH3T3
Vector
B56γ3HA
SS
0 h
9 h
12.5 h
15 h
18 h
24 h
NIH3T3 vector
NIH3T3 B56γ3HA
% of Cells in S phase
Time (h)

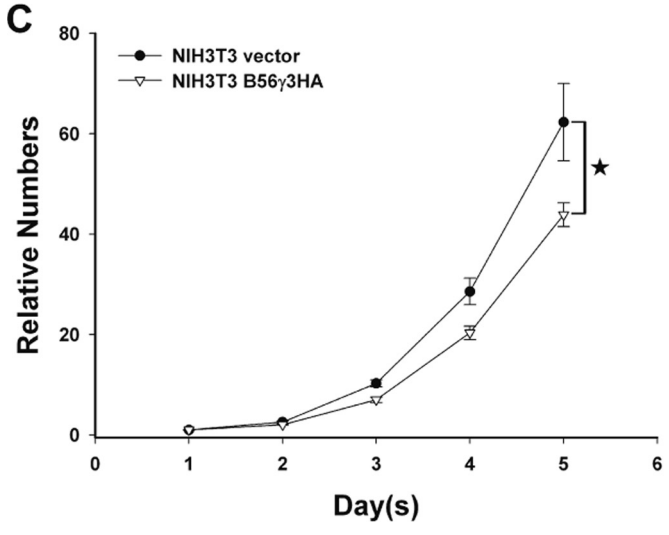
C
NIH3T3 vector
NIH3T3 B56γ3HA
Relative Numbers
Day(s)

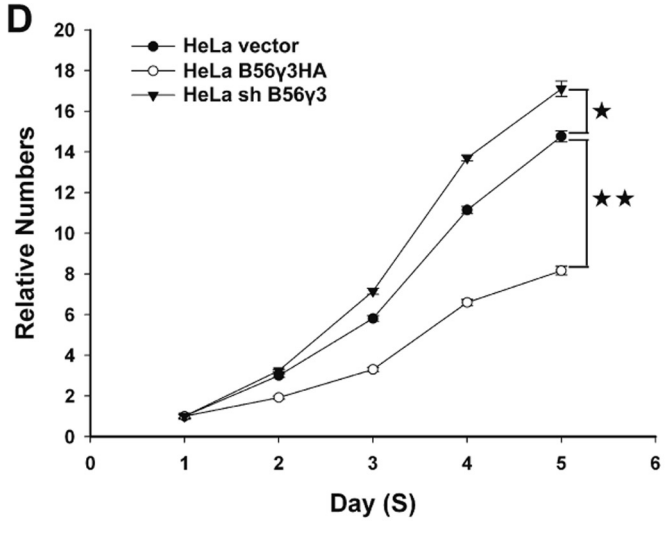
D
HeLa vector
HeLa B56γ3HA
HeLa sh B56γ3
Relative Numbers
Day (S)

when cells entered S phase (Fig. 4, *B*, *right*, and quantified in *C*). Taken together, the results indicate that the B56γ regulatory subunits, at least B56γ2 and B56γ3, play a crucial role in the S phase-specific increase of nuclear localization of PP2A holoenzymes.

The B56γ Subunits Regulate Nuclear PP2A Activity That Is Increased in an S Phase-specific Manner—Because we found that overexpression of B56γ3 results in elevated nuclear localization of PP2A A and C subunits, we asked whether overexpression of B56γ3 affects nuclear PP2A activity. By pulling down PP2A of the nuclear extracts and assessing the catalytic activity using a phosphopeptide substrate *in vitro*, we found that nuclear PP2A activity was increased by overexpression of B56γ3 in NIH3T3 cells (Fig. 5*A*). Next, we measured nuclear PP2A activity during S phase entry in NIH3T3 cells overexpressing B56γ3. PP2A activity was increased near 40% at the G_1-S boundary and in S phase as compared with that of steady-state NIH3T3 cells (Fig. 5*B*). Furthermore, we investigated the role of endogenous B56γ3 on regulating nuclear PP2A activity during progression into S phase in HeLa cells. Consistent with results of biochemical fractionation (Fig. 4*B*), HeLa cells with control knockdown (shLuc) exhibited a near 2-fold increase in nuclear PP2A activity during progression into S phase (Fig. 5*C*, *left*). Knockdown of B56γ3 expression alone significantly blocked the increase in nuclear PP2A activity at the G_1/S border and in S phase (Fig. 5*C*, *middle*). When expression of both B56γ2 and B56γ3 was knocked down, the increase in nuclear PP2A activity at the G_1/S border and in S phase was completely abolished (Fig. 5*C*, *right*). Together these results demonstrate that the B56γ subunits, at least B56γ2 and B56γ3, are responsible for S phase-specific increases in nuclear PP2A activity.

B56γ3 Regulates the G_1 to S Transition of the Cell Cycle and Regulates p27KIP1 Levels—The finding that B56γ3 is enriched in the nucleus during progression into S phase prompted us to investigate whether B56γ3 plays a role in cell cycle progression at the G_1/S transition. We analyzed cell cycle re-entry of NIH3T3 cells with or without B56γ3 overexpression that were arrested in G_0/G_1 by serum starvation (Fig. 6*A*) or contact inhibition (Fig. 6*B*) and subsequently stimulated with 10% serum or replated at low density, respectively, to re-enter the cell cycle. Cell cycle profiles of cells arrested in G_0/G_1 and in various time points after serum replenishment or replating at low density were assessed by PI staining for the DNA content in conjunction with fluorescence-activated cell sorter analysis. As shown in Fig. 6*A*, both NIH3T3 cells with vector only and B56γ3 overexpression were arrested in G_0/G_1 (near 97%) by serum starvation, and no difference in the kinetics of cell cycle progression was found between these cells by 13 h after serum stimulation (Fig. 6*A*). Nevertheless, after 15 h after serum stimulation, cells overexpressing B56γ3 started to show a significantly lower increase in S phase cells (34.73%) compared with cells with vector only (50.11%), and not until 18 h after serum stimulation did the cells overexpressing B56γ3 accumulate S phase populations comparable with that of cells with vector only. Similarly, 12.5 h after released from contact inhibition, NIH3T3 cells overexpressing B56γ3 began to show a lower increase in S phase cells compared with cells with vector only (Fig. 6*B*), and significantly reduced populations of S phase cells were found in cells overexpressing B56γ3 compared with control cells up to 18 h after released from G_0/G_1 arrest (Fig. 6*B*). The delay of the G_1 to S transition by B56γ3 overexpression is a very specific effect of B56γ3 as we did not see the same phenomenon in cells overexpressing B55α (data not shown). As we found increased *in vitro* PP2A catalytic activity toward a phosphopeptide substrate in the nuclear extracts of NIH3T3 cells overexpressing B56γ3 and in cells progressing into S phase (Fig. 5), we hypothesized that increased nuclear PP2A catalytic activity mediated by B56γ3 overexpression may dephosphorylate specific phosphorylated molecules involved in cell cycle control during the transition form G_1 to S phase. Among known molecules involved in this control, p27KIP1 (hereafter referred to as p27), a cyclin-dependent kinase inhibitor, has been linked to control of cell cycle transition from G_0, G_1, into S phase in quiescent cells arrested by serum starvation, contact inhibition, or transforming growth factor-β treatment (27–31). We, therefore, investigated whether B56γ3 overexpression affects p27 protein levels when quiescent cells were re-stimulated to enter the cell cycle. As shown in Fig. 7, *A* and *B*, higher levels of p27 were detected in cells overexpressing B56γ3 than control cells through the time course when cells were stimulated to re-enter the cell cycle even though levels of p27 were substantially declined when cells progressed into S phase in both control cells and cells overexpressing B56γ3. Consistent with the role of B56γ3 overexpression in up-regulating p27 protein levels in NIH3T3 cells, we found that knockdown of endogenous B56γ3 reduced the p27 protein levels in HeLa cells (Fig. 7*C*). Because cyclin E/CDK2-catalyzed phosphorylation of Thr-187 of p27 mediates degradation of p27 in late G_1 and S phase cells (32–36), we investigated whether B56γ3 may play a role in regulating Thr-187 phosphorylation of p27 and subsequently affect the turnover of p27. As shown in Fig. 7*A*, substantially higher levels of Thr-187 phosphorylation were seen at 14 h and later time points after serum stimulation in control cells than that of overexpressing B56γ3 (Fig. 7*A*). In parallel, we found reduced levels of phosphorylation at Thr-187 of p27 in cells overexpressing B56γ3 as compared with that of control cells through the time course after released from contact inhibition (Fig. 7*B*). We further determined the relationship between B56γ3-containing PP2A holoenzymes and p27. We first performed co-immunoprecipitation analysis and found that HA-tagged B56γ3 and the endogenous PP2A A and C subunits were detected in the immunocomplexes of FLAG-tagged p27 (Fig.

FIGURE 6. **B56γ3 regulates the G_1 to S transition and cell proliferation.** *A*, NIH3T3 cells with vector only or B56γ3 overexpression were cultured in 0.5% bovine serum for 72 h before stimulation with 10% bovine serum to re-enter the cell cycle. DNA content at the indicated time points was obtained by PI staining and fluorescence-activated cell sorter analyses. Percentages of S phase cells are graphed. Representative data from three experiments with similar results are shown. *B*, NIH3T3 cells with vector only or B56γ3 overexpression were cultured to reach confluence and were subsequently replated at low density to re-enter the cell cycle. DNA content at the indicated time points was analyzed as described above. Percentages of S phase cells are graphed. Representative data from two similar results are shown. NIH3T3 (*C*) or HeLa cells (*D*) with vector, B56γ3 overexpression, or knockdown of B56γ3 were seeded onto 24-well plates, and cell numbers were counted at the time points shown. The difference in relative cell numbers has a p value < 0.05 (*) or < 0.005 (**) by analysis with Student's t test.

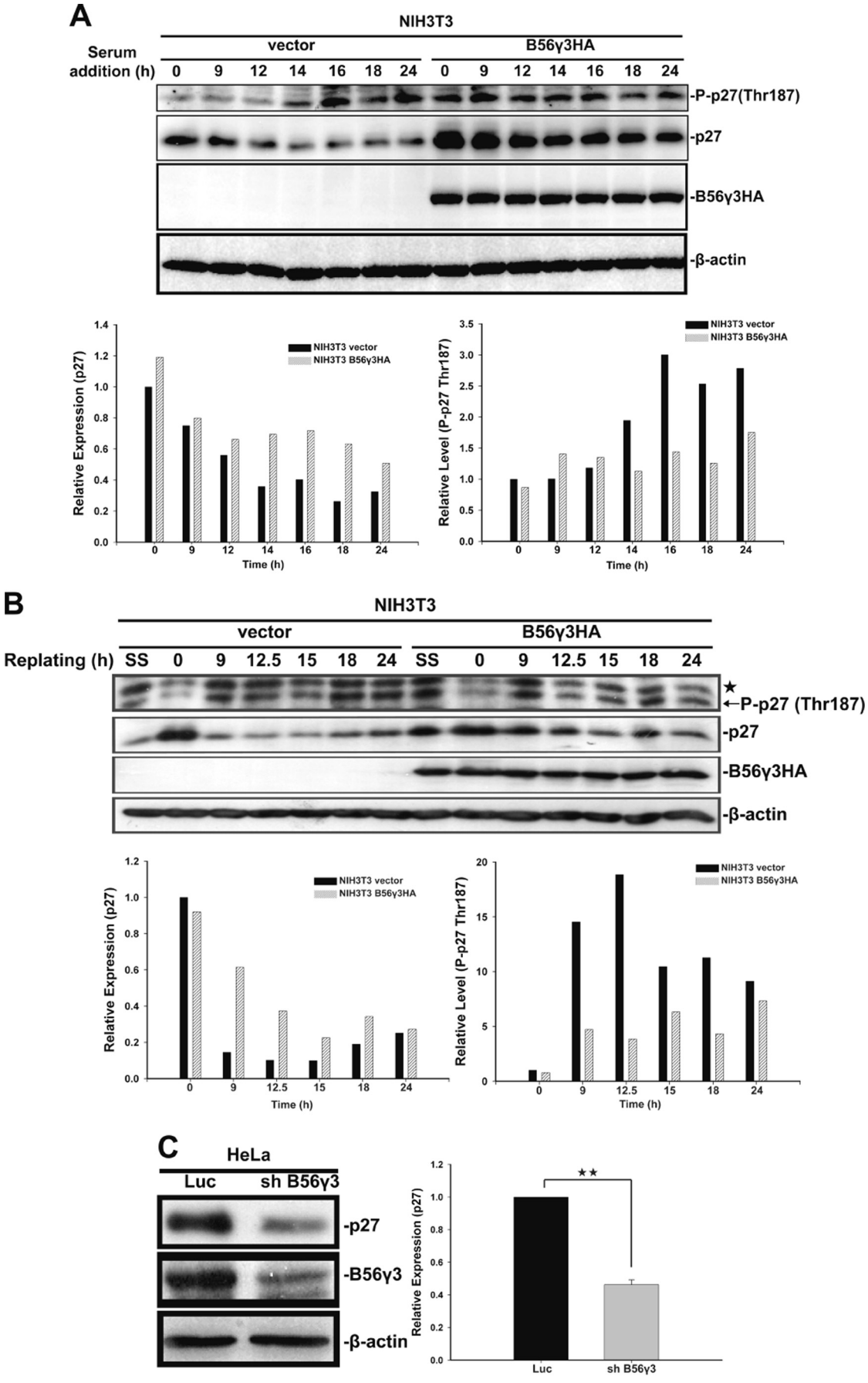
A
NIH3T3
vector
B56γ3HA
Serum addition (h)
0 9 12 14 16 18 24 0 9 12 14 16 18 24
-P-p27(Thr187)
-p27
-B56γ3HA
-β-actin
Relative Expression (p27)
NIH3T3 vector
NIH3T3 B56γ3HA
Time (h)
Relative Level (P-p27 Thr187)
B
NIH3T3
vector
B56γ3HA
Replating (h)
SS 0 9 12.5 15 18 24 SS 0 9 12.5 15 18 24
★
←P-p27 (Thr187)
-p27
-B56γ3HA
-β-actin
C
HeLa
Luc
sh B56γ3
-p27
-B56γ3
-β-actin
Relative Expression (p27)
★★

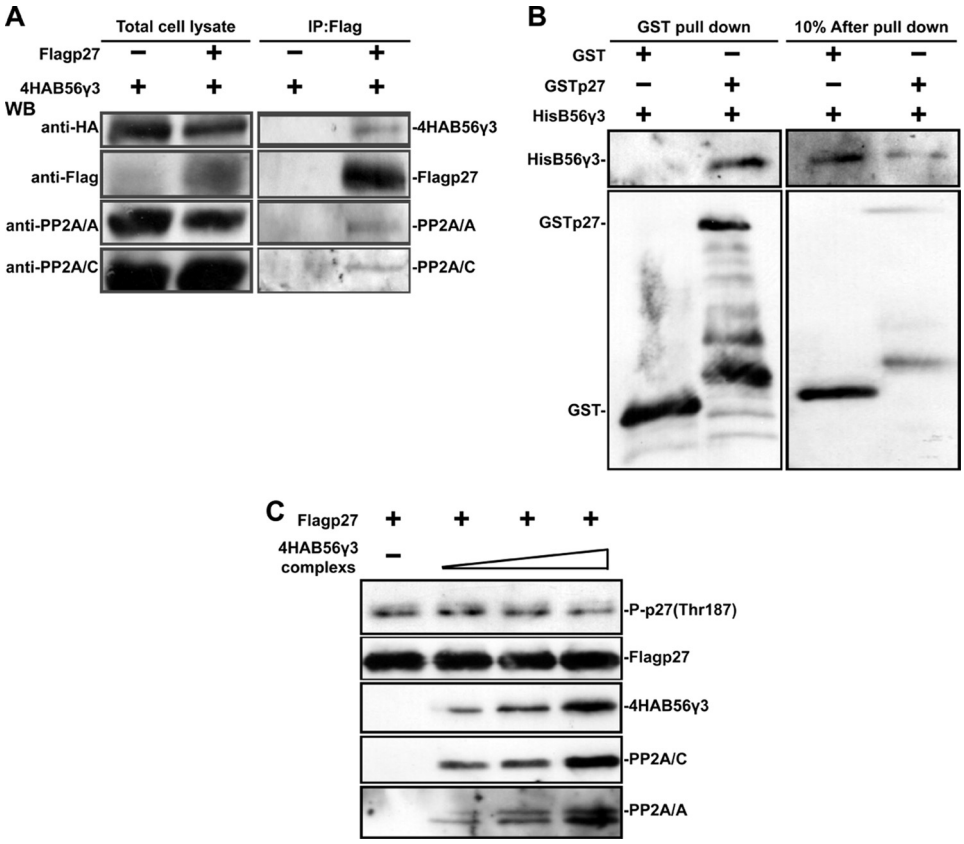

FIGURE 8. **The B56γ3-containing PP2A holoenzyme associates with p27 and catalyzes dephosphorylation of phospho-p27 (Thr-187).** *A*, lysates of NIH3T3 cells co-transfected with pcDNA3.1–4HAB56γ3 and pBMN-IRES-EGFP-FLAG-p27 or empty vector were immunoprecipitated (*IP*) by anti-FLAG-Sepharose, and the immunocomplexes were analyzed by SDS-PAGE and Western blotting (*WB*) by specific antibody as indicated. *B*, *in vitro* pulldown analysis was carried out by mixing 2 μg of recombinant GST or GST-p27 with 2 μg of recombinant His-B56γ3 and incubating at 4 °C for 4 h. GST pulldown assays were then analyzed by SDS-PAGE and specific antibodies for GST and B56γ3. Ten percent of mixed recombinant proteins after pulldown analysis were loaded and detected as a control. *C*, dephosphorylation reactions of phospho-p27 (Thr-187) in the absence or presence of various amounts of B56γ3-containing PP2A complexes were preformed as described under "Experimental Procedures." Expression levels of phospho-p27 (Thr-187), FLAGp27, 4HAB56γ3, and PP2A A and C subunits were detected by Western blotting by antibodies described earlier.

8*A*). Reciprocally, FLAG-tagged p27 was co-precipitated with the immunocomplexes of HA-tagged B56γ3 (supplemental Fig. 4). We next investigated if B56γ3 can directly interact with p27 by *in vitro* pulldown analysis using recombinant GST or GST-p27 proteins to interact with recombinant His-B56γ3 proteins. After pulldown of GST or GST-p27 using glutathione-Sepharose, we found that His-B56γ3 proteins were associated with GST-p27 but not with control GST proteins (Fig. 8*B*). Furthermore, we examined whether B56γ3-containing PP2A holoenzymes catalyze dephosphorylation of the phospho-Thr-187 of p27 by performing *in vitro* dephosphorylation analysis. As shown in Fig. 8*B*, a high dose of B56γ3-containing PP2A holoenzymes dephosphorylated the phospho-Thr-187 of p27 *in vitro*. Furthermore, we investigated the role of B56γ3 in cell proliferation in both NIH3T3 and HeLa cells as it regulated p27 levels and the G_1 to S transition. B56γ3 overexpression reduced cell number by day 5 by ~25% in both NIH3T3 and HeLa cells (Fig. 6, *C* and *D*), and the reduction in cell number did not result from increased cell death (data not shown), whereas an ~16% increase in cell number was found by day 5 in HeLa cells with knockdown of B56γ3 (Fig. 6*D*). These results suggest that B56γ3-containing PP2A holoenzymes regulate Thr-187 phosphorylation and turnover of p27 and regulate the G_1 to S transition.

DISCUSSION

Studies in yeast showed dynamic and distinct patterns of subcellular localization of the B subunits of PP2A throughout the cell cycle. Now we reveal the dynamic intracellular redistribution of the PP2A B56γ3 regulatory subunit in mammalian cells. We show that redistribution of B56γ3 between the cytosol and nucleus is regulated in a cell cycle-specific manner using immunostaining (Fig. 1). Similarly, biochemical fractionation analysis unveils that B56γ3 localizes in both the nucleus and cytoplasm and that B56γ3 is increased significantly in the nucleus in cells progressing into S phase (Figs. 3 and 4). It has been believed that the B regulatory subunits determine the subcellular localization and activity of PP2A holoenzymes. Here, we demonstrate that overexpression of B56γ3 leads to an increase in nuclear distribution of A and C subunits (Figs. 2 and 3) and elevated nuclear PP2A activity (Fig. 5). We also found an S phase-specific increase in endogenous nuclear PP2A A and C subunits and nuclear PP2A activity in both NIH3T3 and HeLa cells. Knockdown of the endogenous B56γ2 and B56γ3 subunits significantly reduces S phase-specific

FIGURE 7. **B56γ3 regulates p27 phosphorylation and p27 protein levels.** *A*, NIH3T3 cells with vector only or B56γ3 overexpression were serum-starved and re-stimulated with 10% bovine serum to re-enter the cell cycle. Cell lysates were collected at the times indicated after serum replenishment and analyzed by SDS-PAGE and Western blotting by specific antibodies for phospho-p27 Thr-187, total p27, HA tag, and β-actin. *B*, NIH3T3 cells with vector only or B56γ3 overexpression were cultured to reach confluence and were subsequently replated at low density to re-enter the cell cycle. Cell lysates were collected at the times indicated after replating and analyzed by SDS-PAGE and Western blotting by specific antibody as described above. The *asterisk* indicates a nonspecific band. The *arrow* indicates phospho-p27 (Thr-187). The relative levels of p27 and phospho-p27 (Thr-187) were quantified by densitometry and normalized with β-actin and with both total p27 and β-actin, respectively. *C*, lysates of HeLa cells expressing vector only or an shRNA specifically targeting B56γ3 (shB56γ3) were analyzed for the expression of p27, B56γ3, and β-actin. The relative levels of p27 were quantified by densitometry and normalized with β-actin. Results were expressed as relative p27 expression level *versus* that of cells with control shLuc knockdown at steady state, which was set as 1. Data are shown as the means ± S.D. of three experiments. The differences of p27 levels between B56γ3 knockdown and the control cells were assessed for statistical significance by Student's *t* test with p value < 0.005 (**).

increase in nuclear localization of the A and C subunits and abrogates S phase-specific increase in nuclear PP2A activity.

Correlation between the Localization of B56γ3, A, and C Subunits—By immunostaining and biochemical fractionation analyses, we confirmed that overexpression of B56γ3HA increased nuclear distribution of endogenous A and C subunits (Figs. 2 and 3 and supplemental Fig. 2). Intriguingly, increased cytoskeletal staining of the A subunit was observed in both NIH3T3 and HeLa cells overexpressing B56γ3 (Fig. 2 and supplemental Fig. 2). However, we did not observe a similar cytoskeletal staining pattern of the B56γ3 or C subunit. There are a few possible reasons that might cause this discrepancy. For example, the cytoskeletal localized B56γ3 or C subunit is inaccessible for recognition by the antibody applied here because of epitope masking. In addition, although we found that exogenous B56γ3HA integrated into the holoenzyme complex by associating with the endogenous A and C subunits (supplemental Fig. 3), increased cytoskeletal localization of the A subunit is probably not a direct targeting function of B56γ3 and is probably caused by B56γ3-modulated upstream signaling pathways involved in regulating cytoskeletal rearrangement. In support of this, B56γ1, highly homologous to B56γ3, was shown to localize to focal adhesions and is associated with paxillin to regulate the actin network (12). Furthermore, results of biochemical fractionation analyses showed that knockdown of both B56γ2 and B56γ3 resulted in a more reduction of the S phase-specific increase (near completely abolished) in the nuclear A and C subunits as compared with that caused by knockdown of B56γ3 alone (Fig. 4), suggesting other B subunits in addition to B56γ3 in regulating the S phase-specific accumulation of the nuclear A and C subunits. In support of this, B56γ2 similarly accumulated in the nucleus during cells progressing into S phase (Fig. 4*B*). Nevertheless, we cannot rule out the possibility that a better knockdown efficiency of B56γ3 (from 60 to 80%) was responsible for abolishing the increase in the nuclear A and C subunits in S phase. Although our data demonstrate that the B56γ subunits play a very crucial role in regulating S phase-specific nuclear enrichment of PP2A holoenzymes, we saw a negligible effect on steady-state nuclear distribution of A and C subunits by knockdown of both B56γ2 and B56γ3 (Fig. 4), suggesting that multiple B subunits control steady-state nuclear localization of PP2A and that the decrease of nuclear localization of A and C subunits due to knockdown of B56γ2 and B56γ3 is likely compensated by other nuclear targeting B subunits.

Regulation of Nuclear Localization of B56γ3—Although we provide evidence here to demonstrate that B56γ3 influences the distribution of PP2A AC core enzymes in the nucleus in a cell cycle-specific manner, the exact mechanism underlying nuclear localization of B56γ3-containing PP2A holoenzymes is largely unknown. Nuclear import of larger molecules is usually controlled by a nuclear localization signal and importin-mediated mechanism (37, 38). There are at least four candidate classical nuclear localization signals found in B56γ3 by sequence analysis,[3] suggesting that B56γ3 may enter the nucleus through the classical nuclear localization signal- and importin α-dependent mechanism. Moreover, crystal structure of B56γ1 reveals that B56γ1 is structurally similar to importin α (39). Based on the high homology between B56γ1 and B56γ3, these data suggest that B56γ3 may also enter the nucleus independent of importin α. Furthermore, a previous report (40) showed that the A subunit alone interacts with importin 9 and importin β, which belong to the transport receptor karyopherin β family. Therefore, it is possible that the complex formed between the A and B56γ3 subunits cooperatively targets the PP2A holoenzyme to the nucleus. In addition, the mechanism underlying the S phase-specific nuclear enrichment of B56γ3-containing PP2A is unclear. It is possible that at the G_1/S border, nuclear import of B56γ3 is increased significantly or that the export of B56γ3 out of the nucleus is slowed down to render nuclear accumulation of B56γ3-containing PP2A. Signaling stimulations that cause a shift in the direction of nuclear transport of many signal transducers by mechanisms of post-translational modification have been demonstrated (37). We observed a slight band shift of both the endogenous (Fig. 4*B*) and exogenous B56γ3 (Fig. 3*A*) on SDS-PAGE that was extracted from the nuclear fraction compared with that of the cytoplasm. We propose that B56γ3 is post-translationally modified before or after entering the nucleus in a cell-cycle specific manner and that the specific modification either promotes nuclear import of B56γ3 or retains B56γ3 in the nucleus.

B56γ3-containing PP2A Holoenzymes Regulate the G_1 to S Transition, p27 Protein Levels, and Cell Proliferation—We found that B56γ3 overexpression inhibits the proliferation of both NIH3T3 and HeLa cells, whereas silencing B56γ3 promotes the proliferation of HeLa cells. In support of this antiproliferative activity of B56γ3, we showed that B56γ3 overexpression delays the G_1 to S transition in NIH3T3 cells (Fig. 6). B56γ3 was shown to inhibit cell proliferation in a p53-dependent manner, and it was shown that B56γ3 targets PP2A holoenzymes to dephosphorylate p53 at Thr-55 in response to DNA damage, resulting in p53 stabilization and cell cycle G_1 arrest (21). We showed that B56γ3 overexpression reduces levels of p27 phosphorylation at Thr-187, resulting in enhanced p27 levels, whereas knockdown of endogenous B56γ3 reduces p27 levels (Fig. 7). Results of co-immunoprecipitation and *in vitro* pulldown analysis (Fig. 8) further suggest that B56γ3-containing PP2A holoenzymes may directly interact with p27 in cells. Moreover, B56γ3-containing PP2A holoenzymes dephosphorylate phospho-p27 at Thr-187 *in vitro* (Fig. 8). Thus, in addition to p53, our data suggest that B56γ3 directs PP2A holoenzymes to regulate p27 phosphorylation at Thr-187 and modulates p27 protein turnover during the G_1 to S transition. Nevertheless, we do not rule out the possibility that the B56γ3-containing PP2A holoenzyme dephosphorylates p27 at other phosphorylation sites to stabilize p27 or that the B56γ3-containing PP2A holoenzyme regulates p27 protein levels through other indirect mechanisms. Together, our data demonstrate that B56γ3-containing PP2A holoenzymes regulate p27 protein levels during the G_1 to S transition to monitor cell proliferation and may partly contribute to the tumor suppressor function of PP2A.

[3] T.-Y. Lee, T.-Y. Lai, S.-C. Lin, C.-W. Wu, I.-F. Ni, Y.-S. Yang, L.-Y. Hung, B. K. Law, and C.-W. Chiang, unpublished data.

Acknowledgments—We are grateful to Dr. Marc Mumby for providing the antibody for B56γ, Dr. David Virshup for providing the mammalian expression vector for B56γ3, Dr. Carlos Arteaga for the mammalian expression vector for p27, and Drs. Elizabeth Yang, Brian Wadzinski, Mark Koury, and Nan-Shan Chang for helpful suggestions.

REFERENCES

1. Janssens, V., and Goris, J. (2001) *Biochem. J.* **353,** 417–439
2. Mayer, R. E., Hendrix, P., Cron, P., Matthies, R., Stone, S. R., Goris, J., Merlevede, W., Hofsteenge, J., and Hemmings, B. A. (1991) *Biochemistry* **30,** 3589–3597
3. Healy, A. M., Zolnierowicz, S., Stapleton, A. E., Goebl, M., DePaoli-Roach, A. A., and Pringle, J. R. (1991) *Mol. Cell. Biol.* **11,** 5767–5780
4. McCright, B., and Virshup, D. M. (1995) *J. Biol. Chem.* **270,** 26123–26128
5. Csortos, C., Zolnierowicz, S., Bakó, E., Durbin, S. D., and DePaoli-Roach, A. A. (1996) *J. Biol. Chem.* **271,** 2578–2588
6. Tanabe, O., Nagase, T., Murakami, T., Nozaki, H., Usui, H., Nishito, Y., Hayashi, H., Kagamiyama, H., and Takeda, M. (1996) *FEBS Lett.* **379,** 107–111
7. Moreno, C. S., Park, S., Nelson, K., Ashby, D., Hubalek, F., Lane, W. S., and Pallas, D. C. (2000) *J. Biol. Chem.* **275,** 5257–5263
8. Strack, S., Zaucha, J. A., Ebner, F. F., Colbran, R. J., and Wadzinski, B. E. (1998) *J. Comp. Neurol.* **392,** 515–527
9. Eichhorn, P. J., Creyghton, M. P., and Bernards, R. (2009) *Biochim. Biophys. Acta.* **1795,** 1–15
10. Strack, S., Chang, D., Zaucha, J. A., Colbran, R. J., and Wadzinski, B. E. (1999) *FEBS Lett.* **460,** 462–466
11. Dagda, R. K., Zaucha, J. A., Wadzinski, B. E., and Strack, S. (2003) *J. Biol. Chem.* **278,** 24976–24985
12. Ito, A., Kataoka, T. R., Watanabe, M., Nishiyama, K., Mazaki, Y., Sabe, H., Kitamura, Y., and Nojima, H. (2000) *EMBO J.* **19,** 562–571
13. McCright, B., Rivers, A. M., Audlin, S., and Virshup, D. M. (1996) *J. Biol. Chem.* **271,** 22081–22089
14. Tehrani, M. A., Mumby, M. C., and Kamibayashi, C. (1996) *J. Biol. Chem.* **271,** 5164–5170
15. Gigena, M. S., Ito, A., Nojima, H., and Rogers, T. B. (2005) *Am. J. Physiol. Heart Circ. Physiol.* **289,** H285–H294
16. Kitajima, T. S., Sakuno, T., Ishiguro, K., Iemura, S., Natsume, T., Kawashima, S. A., and Watanabe, Y. (2006) *Nature* **441,** 46–52
17. Tang, Z., Shu, H., Qi, W., Mahmood, N. A., Mumby, M. C., and Yu, H. (2006) *Dev. Cell* **10,** 575–585
18. Jiang, W., and Hallberg, R. L. (2000) *Genetics* **154,** 1025–1038
19. Gentry, M. S., and Hallberg, R. L. (2002) *Mol. Biol. Cell* **13,** 3477–3492
20. Chen, W., Possemato, R., Campbell, K. T., Plattner, C. A., Pallas, D. C., and Hahn, W. C. (2004) *Cancer Cell* **5,** 127–136
21. Li, H. H., Cai, X., Shouse, G. P., Piluso, L. G., and Liu, X. (2007) *EMBO J.* **26,** 402–411
22. Shouse, G. P., Cai, X., and Liu, X. (2008) *Mol. Cell. Biol.* **28,** 448–456
23. Kuo, Y. C., Huang, K. Y., Yang, C. H., Yang, Y. S., Lee, W. Y., and Chiang, C. W. (2008) *J. Biol. Chem.* **283,** 1882–1892
24. Harper, J. V. (2005) *Methods Mol. Biol.* **296,** 157–166
25. Waltregny, D., De Leval, L., Glénisson, W., Ly Tran, S., North, B. J., Bellahcène, A., Weidle, U., Verdin, E., and Castronovo, V. (2004) *Am. J. Pathol.* **165,** 553–564
26. Chiang, C. W., Harris, G., Ellig, C., Masters, S. C., Subramanian, R., Shenolikar, S., Wadzinski, B. E., and Yang, E. (2001) *Blood* **97,** 1289–1297
27. Nourse, J., Firpo, E., Flanagan, W. M., Coats, S., Polyak, K., Lee, M. H., Massague, J., Crabtree, G. R., and Roberts, J. M. (1994) *Nature* **372,** 570–573
28. Polyak, K., Lee, M. H., Erdjument-Bromage, H., Koff, A., Roberts, J. M., Tempst, P., and Massagué, J. (1994) *Cell* **78,** 59–66
29. Polyak, K., Kato, J. Y., Solomon, M. J., Sherr, C. J., Massague, J., Roberts, J. M., and Koff, A. (1994) *Genes. Dev.* **8,** 9–22
30. Toyoshima, H., and Hunter, T. (1994) *Cell* **78,** 67–74
31. Coats, S., Flanagan, W. M., Nourse, J., and Roberts, J. M. (1996) *Science* **272,** 877–880
32. Sheaff, R. J., Groudine, M., Gordon, M., Roberts, J. M., and Clurman, B. E. (1997) *Genes Dev.* **11,** 1464–1478
33. Vlach, J., Hennecke, S., and Amati, B. (1997) *EMBO J.* **16,** 5334–5344
34. Morisaki, H., Fujimoto, A., Ando, A., Nagata, Y., Ikeda, K., and Nakanishi, M. (1997) *Biochem. Biophys. Res. Commun.* **240,** 386–390
35. Montagnoli, A., Fiore, F., Eytan, E., Carrano, A. C., Draetta, G. F., Hershko, A., and Pagano, M. (1999) *Genes. Dev.* **13,** 1181–1189
36. Sutterlüty, H., Chatelain, E., Marti, A., Wirbelauer, C., Senften, M., Müller, U., and Krek, W. (1999) *Nat. Cell Biol.* **1,** 207–214
37. Xu, L., and Massagué, J. (2004) *Nat. Rev. Mol. Cell Biol.* **5,** 209–219
38. Pemberton, L. F., and Paschal, B. M. (2005) *Traffic* **6,** 187–198
39. Xu, Y., Xing, Y., Chen, Y., Chao, Y., Lin, Z., Fan, E., Yu, J. W., Strack, S., Jeffrey, P. D., and Shi, Y. (2006) *Cell* **127,** 1239–1251
40. Lubert, E. J., and Sarge, K. D. (2003) *Biochem. Biophys. Res. Commun.* **303,** 908–913